Soft Matter

PAPER

Temperature-responsive inclusion complex of cationic PNIPAAM diblock copolymer and γ-cyclodextrin†

Giuseppe Lazzara,‡[a] Gerd Olofsson,[a] Viveka Alfredsson,[a] Kaizheng Zhu,[b] Bo Nyström[b] and Karin Schillén*[a]

Aqueous mixtures of γ-cyclodextrin (γ-CD) and the thermosensitive cationic diblock copolymer poly(N-isopropylacrylamide)-b-poly(3-acrylamidopropyl)trimethylammonium chloride (PNIPAAM$_{24}$-b-PAMPTAM(+)$_9$) or the PNIPAAM homopolymer PNIPAAM$_{47}$ have been investigated using various experimental methods. Solid γ-CD–polymer inclusion complexes (pseudopolyrotaxanes) form at ambient temperatures in fairly concentrated CD solutions. The NMR measurements showed that the stoichiometry of the inclusion complexes is close to two NIPAAM units per CD molecule. The cationic block of the copolymer is not incorporated into the CD cavity. Synchrotron radiation X-ray diffraction spectra of the solid inclusion complexes indicate a compact columnar structure of CD molecules threaded onto the PNIPAAM chains. In water, square-shaped cyclodextrin aggregates were found to co-exist with single cyclodextrin molecules. In mixed solutions of γ-CD and PNIPAAM$_{24}$-b-PAMPTAM(+)$_9$ these aggregates disintegrate with time as inclusion complexes are formed and the kinetics was studied using time-resolved static and dynamic light scattering and cryo-TEM. Steady-state fluorescence spectroscopy measurements reveal that the CD molecules dethread from the PNIPAAM chains upon increasing the temperature to 40 °C, which is above the lower critical solution temperature of PNIPAAM.

Introduction

The word polyrotaxane is generally used to identify supramolecular structures that are formed by a linear axis (the polymer chain) with several ring-shaped molecules like cyclodextrin (CD) threaded onto it.[1] The structures have bulky moieties bound to each end of the polymer chain so that the ring molecules cannot dethread due to steric constraint. If there are no stoppers at the end of the polymer chains, the word pseudopolyrotaxane is used. The net attractive intermolecular interactions behind this type of inclusion complex formation are hydrophobic interaction and van der Waals forces.[2–4] The pseudopolyrotaxanes and polyrotaxanes formed by block copolymers and CD molecules are extensively investigated because they have tunable structures and they can be used in several application fields based on molecular

recognition and molecular switches.[1,5] Thorough control of such supramolecular structures by using external stimuli and the understanding of the involved mechanisms is a challenge for the design of smart nanomaterials.[3]

The CDs are cyclic oligosaccharides formed by glucopyranose units. They have a truncated cone shape with a hollow cavity, which may incorporate hydrophobic solutes or polymer chains. It has been observed that several CD rings can thread a polymer chain assuming either a close compact[1,6] or a loose[6] structure depending on the nature of the CD. If copolymers are considered, the size of the CD cavity determines which block will be enclosed. Moreover, Fujita et al.[7] reported that the CD can be moved from one block to another by varying the temperature.

It is interesting to note that CD molecules in water have a tendency to form clusters,[8–10] which have been considered strategic in the formation of pseudopolyrotaxanes. The formation of an inclusion complex between Nylon-6 and α-CD has been used to manipulate the polymorphic crystal structure, crystallinity and subsequent orientation of the polymer chain.[11] Furthermore, it has been shown that supramolecular inclusion complexes with CD can control the unwinding and rewinding of a double helix of oligoresorcinol,[12] the stretching of polymer brushes[13] and the formation of functional pseudopolyrotaxanes for drug and gene delivery.[14,15] Promising results in the field of nanoelectronics have been presented by CD-threaded polymers.[16]

[a]Division of Physical Chemistry, Department of Chemistry, Center for Chemistry and Chemical Engineering, Lund University, P.O. Box 124, SE-221 00 Lund, Sweden. E-mail: Karin.Schillen@fkem1.lu.se
[b]Department of Chemistry, University of Oslo, P.O. Box 1033, Blindern, N-0315 Oslo, Norway

† Electronic supplementary information (ESI) available: Chemical shifts for γ-CD protons in the presence of polymers. Time-resolved SLS data for an aqueous mixture of 10 wt% γ-CD and 1 wt% PNIPAAM$_{72}$. Time-resolved SLS and DLS data for an aqueous mixture of 10 wt% γ-CD and 0.5 wt% PNIPAAM$_{24}$-b-PAMPTMA(+)$_9$. See DOI: 10.1039/c2sm07252a

‡ Present address: Department of Chemistry, University of Palermo, Viale delle Scienze, IT 90128 Palermo, Italy.

It is known that CDs can influence the aggregation of thermoresponsive copolymers.[17–22] The lower critical solution temperature (LCST) of poly(N-isopropylacrylamide) (PNIPAAM) moieties can be tuned if proper substituent groups that can be enclosed by CD are introduced.[18,23] To the best of our knowledge there are no reports on CD threading PNIPAAM polymer chains. It is worth noting that inclusion complex formation can occur between PNIPAAM and the smaller β-CD if polymerization of the NIPAAM monomer is performed in the presence of β-CD.[24] In principle, the use of a polymer with the ability to self-assemble in the presence of CDs can provide a way to a specific control of self-assembled structures of the polymer. With this in mind, we decided to investigate the possibility to form supramolecular structures by mixing γ-CD with a thermosensitive cationic diblock copolymer, poly(N-isopropylacrylamide)-b-poly(3-acrylamidopropyl)trimethyl ammonium chloride, which was synthesized by means of atomic transfer radical polymerization (ATRP). The PNIPAAM homopolymer with varying molar masses was also synthesized and investigated. It was recently shown that diblock copolymers of the same type as those used here are able to form micelles and intermicellar structures in water at temperatures approaching the LCST of the PNIPAAM block.[25] Proton nuclear magnetic resonance (^{1}H-NMR), Fourier transform infrared spectroscopy (FTIR), synchrotron radiation powder X-ray diffraction (SR-PXD), steady-state fluorescence spectroscopy, differential scanning calorimetry (DSC), static and dynamic light scattering (SLS and DLS) and cryo-transmission electron microscopy (cryo-TEM) have been employed to investigate the following aspects: (1) formation and structure of inclusion complexes, pseudopolyrotaxanes, between γ-CD and PNIPAAM homopolymer and cationic diblock copolymer both in solution and in solid state; (2) response to temperature changes of the obtained supramolecular structures; and (3) effect of the copolymer on the cyclodextrin aggregates in water.

Results and discussion

When γ-CD and cationic diblock copolymer PNIPAAM$_{24}$-b-PAMPTAM(+)$_9$ and γ-CD and homopolymer PNIPAAM$_{47}$ are mixed in H$_2$O (or D$_2$O, see below) at a fixed polymer concentration of 1 wt% and with variable γ-CD concentration, clear solutions are found up to 14 wt% of γ-CD. Mixtures of 18 wt% γ-CD (still below the solubility limit of γ-CD in H$_2$O or D$_2$O[26]) with PNIPAAM$_{24}$-b-PAMPTAM(+)$_9$ copolymer and PNIPAAM$_{47}$ both at 1 wt% gave a precipitate after ca. 12 h at room temperature after preparation. No precipitate was formed in a mixture of the polymers with α-CD even at a concentration close to its solubility limit.[26] Moreover, the aqueous mixture of the longer PNIPAAM homopolymer (PNIPAAM$_{72}$) (1 wt%) and γ-CD (18 wt%) did not show any precipitation after more than one week. According to the literature,[2,27–31] pseudopolyrotaxanes often occur as water-insoluble crystalline precipitates although water-soluble inclusion CD–polymer inclusion complexes also exist.[5] Lo Nostro et al.[2] have proposed that precipitation is caused by attractive forces that appear due to differences in spatial dielectric properties (in the parallel direction compared to those in the perpendicular direction of the long axis of the polyrotaxane), which in turn originate from the forced

stretching of the linear polymer within the tubular structure of the CD molecules. The precipitates were separated by centrifugation at 4000 rpm, rinsed with cold water (4 °C) several times, dried under vacuum for 24 h and thereafter analyzed using FTIR and synchrotron radiation powder X-ray diffraction. The solution properties of the CD–polymer mixtures were investigated by ^{1}H-NMR, fluorescence and calorimetric techniques and by dynamic and static light scattering. Finally, by using cryo-TEM a visual view of the solutions at different times was achieved. The results of the ^{1}H-NMR measurements are discussed first.

^{1}H-NMR in aqueous solution

NMR is a useful technique for the determination of the stoichiometry of CD–polymer inclusion complexes.[1,27,32] Moreover, the chemical shifts in D$_2$O of strategically selected protons of the guest and of cyclodextrin molecules can be used to prove the formation of inclusion complexes.[33] With this aim we measured the ^{1}H-NMR spectra of γ-CD–PNIPAAM$_{24}$-b-PAMPTAM(+)$_9$ and γ-CD–PNIPAAM$_{47}$ mixtures in D$_2$O. The polymer concentration was fixed to 1 wt% and with variable γ-CD concentration up to 14 wt%. In this concentration regime the solutions were clear without indication of precipitation (as described above).

Fig. 1 presents two representative ^{1}H-NMR spectra obtained for the PNIPAAM$_{24}$-b-PAMPTAM(+)$_9$ copolymer and for the γ-CD–PNIPAAM$_{24}$-b-PAMPTAM(+)$_9$ mixture in D$_2$O, and from which proton-chemical shifts are determined. Fig. 2 illustrates the dependence of the chemical shift of some key protons in the polymer chain on the γ-CD concentration. The δ changes are rather small but still they clearly show that the addition of γ-CD generates an almost linear increase of δ values for H[8] but does not alter the chemical shift of H[14] (for notations, see Chart 1). Assuming the shifts to vary linearly with concentration, the error in the slopes is estimated to about 4.5%. Therefore, both the PNIPAAM block of the copolymer and the PNIPAAM homopolymer (H[8]) interact with cyclodextrin whereas the
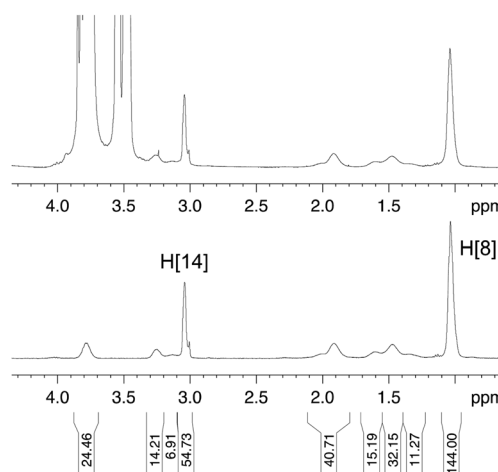

Fig. 1 ^{1}H NMR spectra of 1 wt% PNIPAAM$_{24}$-b-PAMPTAM(+)$_9$ copolymer in D$_2$O (bottom) and in the presence of 14 wt% γ-CD (top) at 25 °C. The proton integrals are given for the copolymer. The ^{1}H nuclei are marked with numbers according to Chart 1. The HDO peak (δ = 4.7 ppm) is not shown.
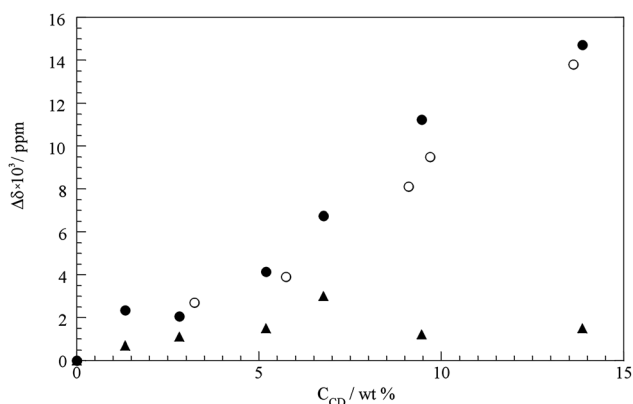
Fig. 2 Changes in the chemical shift obtained from ^{1}H-NMR as a function of γ-CD concentration for the H[14] (triangles) and H[8] (circles) nuclei. Filled and empty symbols refer to the copolymer and PNIPAAM$_{47}$, respectively. ^{1}H nuclei numbers are according to Chart 1.
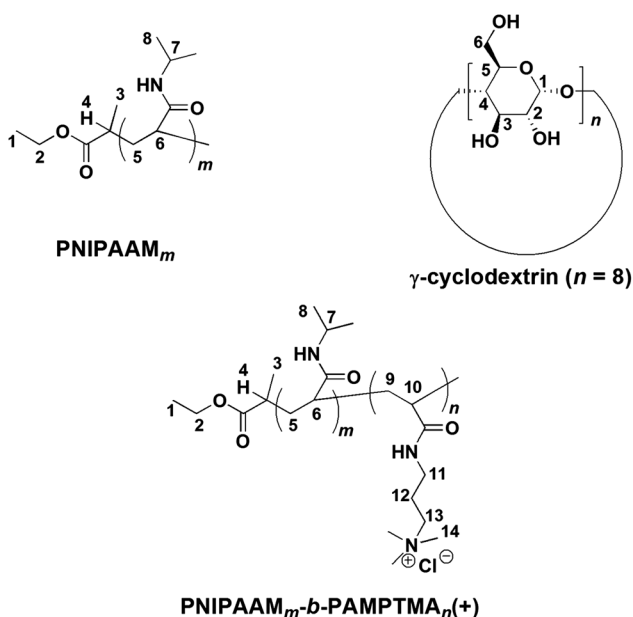

Chart 1 Molecular structure and numbering scheme for the ^{1}H nuclei of the polymers investigated in this study: poly(N-isopropylacrylamide) homopolymers PNIPAAM$_m$ (m = 47 and 72), γ-cyclodextrin and cationic diblock copolymers of PNIPAAM and poly(3-acryl-amidopropyl)trimethylammonium chloride (PAMPTAM(+)), PNI-PAAM$_{24}$-b-PAMPTAM(+)$_9$ and PNIPAAM$_{26}$-b-PAMPTAM(+)$_{15}$.

cationic block (H[14]) does not. The nearly constant chemical shift for the H[14] as a function of the CD concentration rules out that the changes in the δ values for H[8] are just a solvent effect. Based on these findings, we propose that the homopolymer chain, as well as the PNIPAAM block of the copolymer, are enclosed and, thus, that γ-CD is block-selective. This picture reflects the bulky nature of the cationic block and the geometric compatibility of the PNIPAAM chain with the γ-CD cavity as expected on the basis of the van der Waals volume[34] and the monomer length.[35]

It should be noted that the δ values for H[8] of both polymers do not reach a plateau (Fig. 2) even at the highest γ-CD

concentration (note that even higher cyclodextrin concentrations lead to precipitation). As judged from the measurements, the threading process does not go to completion within the 24 h period after preparation of the mixed solutions.

In principle, the inclusion of a certain compound into the CD cavity can also be monitored by observing the chemical shift of protons in the γ-CD cavity (H[3] and H[5]). However, it has been shown[36–39] that at high CD concentration, which is the case here, all of the protons from the CD molecule show a change in δ due to the formation of self-assembled structures (see below). For this reason, the interpretation of the chemical shifts of the CD protons is not straightforward being a combination of CD cluster formation (observed by DLS and cryo-TEM) and CD–polymer interactions. In our case, all of the CD protons show similar δ vs. concentration profiles in solutions with and without polymer (see ESI†).

The solubility of the precipitates formed by mixing solutions of 18 wt% γ-CD and 1 wt% PNIPAAM$_{24}$-b-PAMPTAM(+)$_9$ copolymer or PNIPAAM$_{47}$ was also analyzed by ^{1}H-NMR. The precipitate from the block copolymer mixture remained essentially insoluble in water (H$_2$O or D$_2$O) at least for two days even if a small amount of the material was dispersed (0.1 wt%). However, if such a solid–liquid two-phase mixture is warmed to 40 °C it becomes instantaneously a clear solution and remains clear after cooling to room temperature. It is reasonable to assume that the precipitate is in principle only composed of inclusion complexes in a crystalline form. Therefore it was of interest to also analyze the obtained γ-CD–PNIPAAM$_{24}$-b-PAMPTAM(+)$_9$ one-phase D$_2$O solution by means of ^{1}H-NMR. Since signals from both γ-CD and copolymer were present, the stoichiometry could be determined from their integrals. A NIPAAM monomer to γ-CD (NIPAAM/γ-CD) molar ratio of 1.95 was found. This is in a good agreement with the calculated stoichiometry of 1.98 obtained by assuming that the cationic block is not incorporated into the γ-CD cavity and that the threaded CD molecules assume a close-packed structure over the PNIPAAM chain. A NIPAAM monomer length of 0.34 nm[35] and a γ-CD cavity depth of 0.7 nm[32] were used for these estimates. It is worth noting that inclusion complex formation can occur between PNIPAAM and the smaller β-CD if polymerization of the NIPAAM monomer is performed in the presence of β-CD.[24]

The precipitate formed from the γ-CD–PNIPAAM$_{47}$ homopolymer mixture was readily soluble in water at room temperature at a concentration of 0.1 wt%. The solution in D$_2$O was investigated by means of ^{1}H-NMR and a NIPAAM/γ-CD molar ratio of 1.90 was obtained. This value agrees well with that obtained for the γ-CD–copolymer mixture. It confirms the close-packed structure of the CDs threaded onto the PNIPAAM chain. Moreover, it shows that the bulky cationic block of the copolymer is not incorporated into the CD cavity.

In order to further investigate the γ-CD–copolymer inclusion complexes, ROESY-NMR was employed on the γ-CD 14 wt% + PNIPAAM$_{26}$-b-PAMPTAM(+)$_{15}$ 1 wt% mixture in D$_2$O. The purpose was to obtain a detailed structure of the inclusion complex from the 2D spectra, see ref. 1 and the references therein. These measurements gave cross-signals both between the γ-CD and the copolymer and within the two separate species. Unfortunately it was not possible to distinguish them apart.
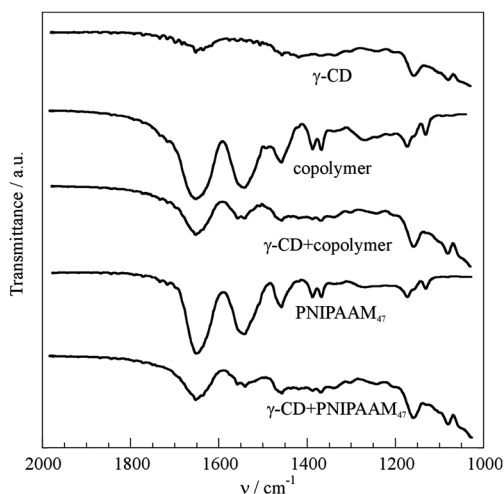
Fig. 3 FTIR spectra of γ-CD, polymers and pseudopolyrotaxanes in the solid state. The bands at about 1540 cm^{-1} and 1650 cm^{-1} are related to the N–H bending and C=O stretching of the PNIPAAM chain, respectively. The double peak at about 1380 cm^{-1} is attributed to the C–H stretching vibration of the methyl groups.

FTIR

FTIR spectra of solid samples of the PNIPAAM$_{24}$-b-PAMP-TAM(+)$_9$ copolymer and PNIPAAM$_{47}$ homopolymer and of the γ-CD–polymer inclusion complexes were recorded (Fig. 3). The bands at ca. 1540 cm^{-1} and 1650 cm^{-1} are ascribed to the N–H bending and C=O stretching of the PNIPAAM chain, respectively.[24] At these wavenumbers the γ-CD spectrum does not show any signal. The confinement of the PNIPAAM into the cavity should alter the N–H signals while the C=O vibration is expected to be unchanged.[24] We observe that the presence of γ-CD generates two effects on the N–H band in the copolymer and the homopolymer systems. Namely, the peak is split into two bands slightly moved towards higher energies while the relative intensity is decreased. Further, the double peak centered at around 1380 cm^{-1} attributed to the C–H stretching vibration of the methyl groups in the isopropyl moiety[40] in the free polymers disappears in the complexes while the C=O band is almost unchanged. Even if this FTIR experiment does not give straightforward evidence for the inclusion of the polymer chain into the CD cavity, it corroborates the results obtained from ^{1}H-NMR.

SR-PXD

In the solid state γ-CD can form two crystal structures called cage and columnar in addition to an amorphous phase.[41,42] Pseudopolyrotaxanes composed of γ-CD and poly(ethylene glycol) (PEG)[43] show a columnar structure and also those composed of γ-CD and poly(butylene carbonate).[31] In our study, precipitates (with a stoichiometric ratio about 2 according to ^{1}H-NMR data) were prepared from aqueous mixtures of γ-CD and polymer (copolymer or PNIPAAM$_{47}$) and dried under vacuum at 25 °C for 72 h. An aqueous γ-CD solution (10 wt%) was evaporated and dried in a similar way. The powder X-ray diffraction patterns are shown in Fig. 4. The γ-CD powder gave diffraction peaks in accordance with the cage-like polymorph.
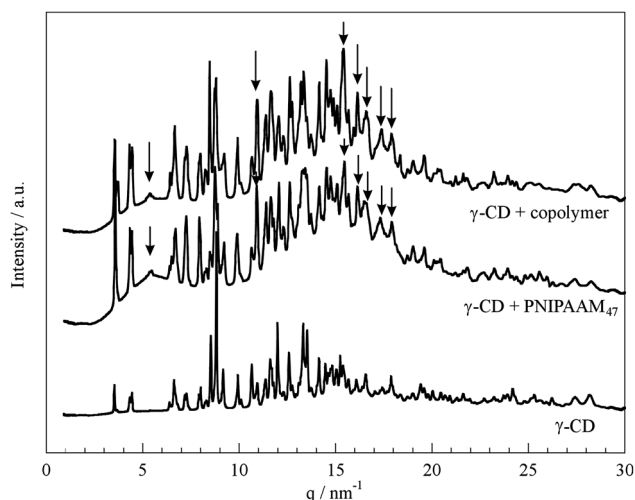

Fig. 4 SR-PXD spectra of γ-CD and pseudopolyrotaxanes in the solid state. The arrows indicate the peaks which appear in the presence of the polymer and that are related to a columnar structure of γ-CD.

Some of the experimental peak positions and the corresponding plane distances are given in Table 1 together with data from the literature.[42] The addition of polymers (either block copolymer or homopolymer) generated new peaks that were all consistent with the columnar structure.[42] The crystallographic spacings for those peaks are given in Table 2. The new peaks have been indexed by means of the EXPO software.[44] The results are consistent with a tetragonal structure, which is in agreement with the columnar structure.[42,43] The derived cell parameters are $a = b = 2.59$ nm, $c = 0.74$ nm for the copolymer system and $a = b = 2.52$ nm, $c = 0.97$ nm for the PNIPAAM$_{47}$ system. The values of a and b are both very close to the values for the columnar structure observed for pure γ-CD (2.37 nm[42]) and for the γ-CD–PEG inclusion complex (2.38 nm[43]) whilst our c parameters of 0.74 nm and 0.97 nm are smaller than those for γ-CD[42] and γ-CD–PEG.[43] 2.29 nm and 1.48 nm, respectively. The c parameter reflects the repeat distance between CDs in the c direction and as the depth of the γ-CD cavity is 0.7 nm,[32] it fits well with the preferred head-to-head and tail-to-tail orientation of CD molecules within the column, see ref. 1. Thus, the X-ray diffraction result agrees with the formation of pseudopolyrotaxanes with a compact CD structure over the PNIPAAM polymer chain as indicated by ^{1}H-NMR. Fig. 5 shows a tentative structure of the γ-CD–copolymer inclusion complex. Values of q derived from the EXPO cell parameters are listed in Table 2 together with the Miller indices. To summarize, we may conclude from the above

Table 1 Crystallographic data for the cage structure of γ-CD^a

q		Spacing
8.82	8.81^b	0.712
11.61	11.71^b	0.541
13.33	13.33^b	0.471
16.57	16.55^b	0.379

^{a} Units are: q, nm^{-1}; spacing, nm. ^{b} Data are from ref. 42 and refer to a cage-like structure.

Table 2 Crystallographic data for the columnar structure of the γ-CD–polymer inclusion complex[a]

q		Spacing	(hkl)
γ-CD–PNIPAAM_{47} inclusion complex			
5.584	5.580[b]	1.125	(210)
11.073	11.067[b]	0.567	(321)
15.526	15.517[b]	0.405	(441)
16.304	16.301[b]	0.385	(402)
16.673	16.678[b]	0.377	(332)
17.459	17.468[b]	0.360	(700)
18.111	18.110[b]	0.347	(512)
γ-CD–PNIPAAM_{24}-b-PAMPTAM(+)_9 inclusion complex			
5.427	5.422[b]	1.158	(210)
10.944	10.948[b]	0.574	(221)
14.752	14.750[b]	0.426	(610)
15.462	—	0.405	—
16.150	16.155[b]	0.389	(441)
17.397	17.405[b]	0.361	(112)
17.916	17.905[b]	0.351	(212)

[a] Units are: q, nm^{-1}; spacing, nm. [b] From EXPO software data analysis.

Fig. 6 (a) Pyrene fluorescence emission spectra (normalized by intensity of the first vibronic peak, I/I_1) in the presence of the precipitate obtained from γ-CD–copolymer aqueous solution at 20 °C (solid line) and 40 °C (dotted line) at 40 min after preparation. (b) The I_1/I_3 ratio obtained from emission spectra at 20 °C (circles) and 40 °C (triangles) as a function of time.
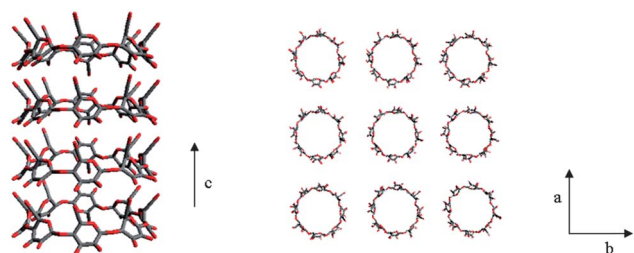

Fig. 5 Tentative structure of the γ-CD–PNIPAAM_{24}-b-PAMPTAM(+)_9 inclusion complex. a and b are the directions in the basal plane and c is the third axis in the tetragonal lattice.

data that our pseudopolyrotaxane solid consists of a disordered crystal with both columnar and cage-like structure. This has also been discussed previously in the recent review on cyclodextrin-based aggregates and inclusion complexes.[9]

Pyrene probe steady-state fluorescence spectroscopy

The dissolution in water of the γ-CD–copolymer pseudopolyrotaxane precipitate upon heating was further investigated to find out whether the dissolution of the inclusion complex leads to the release of CD molecules from the copolymer chain. This aspect was studied by means of fluorescence spectroscopy using pyrene as a probe. The fluorescence technique using the fluorescent chromophore (or probe) pyrene is useful to detect the presence of hydrophobic domains since pyrene is sensitive to the nature of its microenvironment.[45] The ratio between the intensity of the first (at 373 nm) and the third (at 384 nm) vibronic band (I_1/I_3), of the monomer emission spectrum, depends strongly on the polarity of the environment. The ratio is 1.87 in water and it drops down to 0.8 in hydrophobic media.[45] At a block-copolymer concentration in water of 0.1 wt%, the I_1/I_3 ratio for pyrene slightly changed from 1.85 to 1.80 when temperature was varied from 20 °C to 50 °C. However, in 10 wt% of γ-CD in water, the I_1/I_3 ratio obtained was 0.85 due to the incorporation of pyrene molecules into the hydrophobic CD
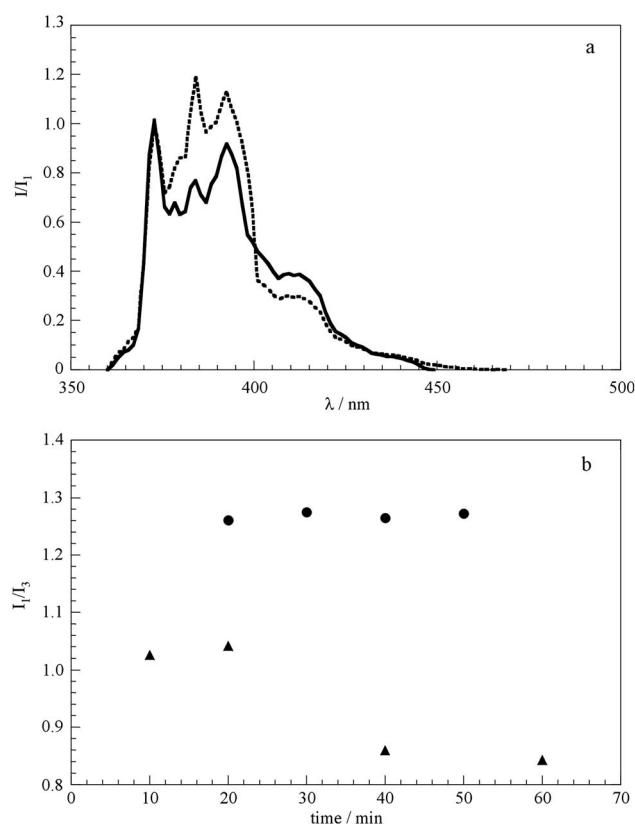
cavity in agreement with the literature.[33] It is thus possible to probe the presence of free γ-CD, not threaded onto the PNIPAAM block of the copolymer, by using pyrene. Therefore, the pseudopolyrotaxane precipitate was placed in a quartz cuvette to which the aqueous pyrene solution was added (the amount of the precipitate in the mixture was 0.1 wt%). The fluorescence emission spectrum of the pyrene was measured as a function of time at 20 °C and 40 °C. A few examples of fluorescence spectra are shown in Fig. 6, together with the time dependence of the I_1/I_3 ratio.

At 20 °C, the I_1/I_3 ratio assumed a constant value of 1.28. The observed I_1/I_3 ratio indicates that the concentration of free γ-CD is large enough to incorporate a fraction of the pyrene molecules but that most of the cyclodextrin is bound in the precipitate. Since the pyrene concentration is low, 5×10^{-7} mol dm^{-3}, the solubility of the precipitate as well as the degree of dissociation (i.e. dethreading) of inclusion complexes that may exist in solution must be low at 20 °C.

Upon heating the solution to 40 °C, where the pseudopolyrotaxane precipitate dissolves, a decrease of the I_1/I_3 ratio with time was observed. We interpret this to be an indication of a dethreading of the γ-CD molecules and subsequent incorporation of the pyrene chromophores into the γ-CD cavities that now are free. After 50 min, the I_1/I_3 ratio assumed the same value

as that measured in the presence of a large excess of γ-CD. Hence, it may be concluded that under these conditions there is enough free γ-CD to incorporate all of the pyrene chromophores. It can be concluded that the dissolution of the pseudopolyrotaxane precipitate leads to the release by dethreading of γ-CD from the copolymer chain at least to such an extent that all pyrene molecules are incorporated. These fluorescence results are also indirect evidence that threading must have occurred at room temperature.

Differential scanning calorimetry

By using DSC it is possible to explore the formation of inclusion complexes between cyclodextrins and polymers in addition to the aggregation of PNIPAAM.[46–48] As a general trend, the formation of copolymer self-assembled structures,[17,19] as well as conventional surfactant micelles,[49,50] is disfavored by cyclodextrin if an inclusion complex is formed with the hydrophobic moiety of the amphiphilic (copolymer or surfactant) component. In the case of polymers, complex formation is easily observed in DSC experiments as an increase in LCST.

A copolymer with a slightly longer cationic block and with similar PNIPAAM block length was used in the DSC experiments (PNIPAAM$_{26}$-b-PAMPTAM(+)$_{15}$). However, since there are no changes in the physical properties, $i.e.$ the LCST, of this copolymer compared to the PNIPAAM$_{24}$-b-PAMPTAM(+)$_9$ copolymer (static light scattering data not shown), the overall conclusion from the DSC investigation is still valid. The DSC thermograms of a 1 wt% PNIPAAM$_{26}$-b-PAMPTAM(+)$_{15}$ copolymer solution and a 10 wt% γ-CD + 1 wt% copolymer aqueous solution are given in Fig. 7. For both solutions, a single endothermic peak was registered from which the enthalpy change for the transition (per mole of copolymer) was determined. The temperature at the onset of the peak, which corresponds to LCST, was also evaluated. Neither the enthalpy change nor the temperature for the transition is sensitive to the addition of γ-CD. In the case of the pure copolymer solution, the enthalpy value is 16.5 kJ mol^{-1} and the onset temperature is 45.6 °C, whereas for the γ-CD–copolymer mixture a value of 16.4 kJ mol^{-1} is obtained at 45.3 °C. Neither has the presence of CD any effect on the PNIPAAM$_{47}$ system. In this case the enthalpy value

is 301 kJ mol^{-1} at 37.9 °C for 1 wt% of homopolymer in water, whereas in the presence of 10 wt% γ-CD a value of 285 kJ mol^{-1} is obtained at 36.6 °C. The large difference between the enthalpy values for the block copolymer and homopolymer systems is due to the electrostatic repulsion between the cationic blocks.

This result is somewhat surprising since we have strong indications of formation of γ-CD–copolymer pseudopolyrotaxanes from the other techniques employed in this study. However, the fluorescence experiments showed that a temperature increase leads to dethreading of cyclodextrin from PNIPAAM. This means that the formation of the inclusion complex observed at 25 °C by means of ^{1}H-NMR is repressed at higher temperatures so that at the LCST the block copolymer is fully free of γ-CD. This explains why the self-assembly process of the copolymer is not affected by the presence of γ-CD.

Dynamic light scattering on binary aqueous solutions

In order to characterize the hydrodynamic size of the diffusive species present in aqueous solutions of γ-CD, PNIPAAM$_{47}$ homopolymer and PNIPAAM$_{24}$-b-PAMPTAM(+)$_9$ copolymer DLS measurements were performed at 25 °C. The measured intensity autocorrelation functions exhibited a fast and a second slower relaxation process in all cases and the corresponding mean relaxation times were obtained from bi-exponential fits from which the apparent hydrodynamic radii $R_{H,app}$ were estimated. Fig. 8 shows three typical bimodal intensity-weighted size distributions obtained from inverse Laplace transformation (ILT) of the correlation functions for aqueous solutions containing 10 wt% of γ-CD, 1 wt% of PNIPAAM$_{47}$ homopolymer and 1 wt% of PNIPAAM$_{24}$-b-PAMPTAM(+)$_9$ copolymer. In the PNIPAAM$_{47}$ case, the fast mode corresponds to the translational diffusion of single homopolymer chains, whereas the slow mode, which has previously been observed for the same molar-mass sample, is associated with the formation of large aggregates and our results are in agreement with the earlier study.[51] The hydrodynamic radius obtained for the fast mode is 1.2 ± 0.1 nm and $R_{H,app}$ of the aggregates is 40 ± 2 nm. PNIPAAM aggregates may form because they have become somewhat hydrophobic since the temperature is not far from the
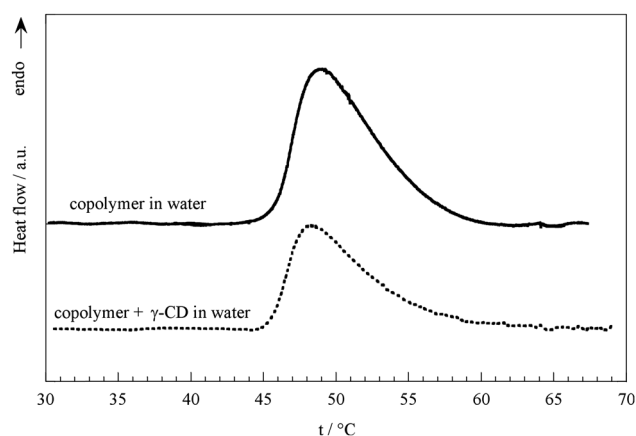

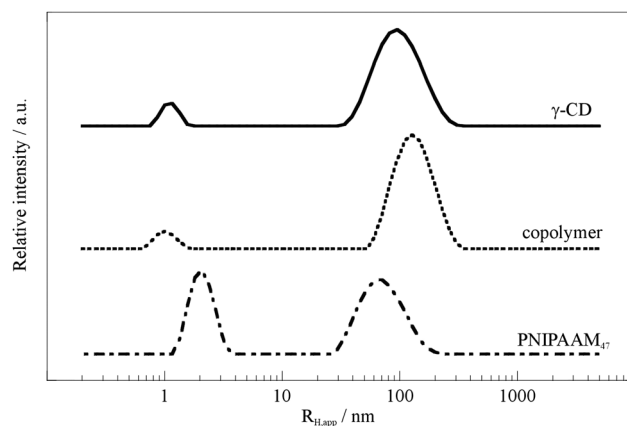**Fig. 7** DSC curves of 1 wt% copolymer in water and in the presence of 10 wt% γ-CD.

Fig. 8 Distributions of the apparent hydrodynamic radii $R_{H,app}$ for 10 wt% γ-CD (—), 1 wt% copolymer (---) and 1 wt% PNIPAAM$_{47}$ (-··-) aqueous solutions at 25 °C.

LCST (about 38 °C). In ref. 51, samples of PNIPAAM with varying molar masses were investigated and it was shown that the formation of aggregates is less pronounced in solutions of PNIPAAM homopolymers of low molar mass such as the one investigated in this study. Their results showed that the hydrophobic interpolymer interactions increase with increasing length of the polymer chains. We observe for the PNIPAAM$_{47}$ solution that the relative area of the slow mode, which corresponds to the pre-exponential amplitude of the bi-exponential intensity autocorrelation function, is almost equal to that of the fast mode (Fig. 8). This indicates that aggregation in this solution is not as extensive as in the other binary solutions that show larger slow modes.

The size distribution of the γ-CD solution shows a bimodal behavior (Fig. 8). The fast mode is attributed to the diffusion of single CD molecules and the second large-amplitude mode to aggregates of γ-CD similar to what has been observed for β-CD in water using DLS.[8,17] The hydrodynamic radii related to the two modes are 1.6 ± 0.1 nm and 59.4 ± 0.6 nm, respectively. The driving force for the CD self-assembly is considered to be the minimization of contact area between domains with different hydrophilicity/hydrophobicity in a CD molecule.[10] These structures are considered to be crucial for the formation of pseudo-polyrotaxanes.[2,8] Lo Nostro et al. have put forward the hypothesis that the pre-aggregates of CD thread the polymer chain all at once during the pseudopolyrotaxane formation.[2]

In the PNIPAAM$_{24}$-b-PAMPTAM(+)$_9$ copolymer case, the fast mode is again linked to the translational diffusion of single copolymer chains with a $R_{H,app}$ of 2.3 ± 0.3 nm. The slow mode indicates that the copolymer chains associate probably due to the amphiphilic properties of the PNIPAAM block as described above. The hydrodynamic radius of the aggregates, 119 ± 1 nm, is somewhat larger than those of the pure homopolymer. Another explanation for the appearance of the second mode could be that it is related to the so-called "slow mode" commonly observed for polyelectrolyte solutions since the copolymer studied in this work is charged.[52] However, this mode will not effect the results obtained related to formation of the inclusion complex.

Time-resolved static and dynamic light scattering

Aqueous stock solutions of γ-CD and the homopolymers, PNIPAAM$_{47}$ and PNIPAAM$_{72}$, and the PNIPAAM$_{24}$-b-PAMPTAM(+)$_9$ copolymer were prepared and mixed in 1 : 1 volume ratio. The final polymer content was 1 wt% and the γ-CD content was 10 wt%. The measurements were carried out by simultaneously measuring DLS and the time-averaged static light scattering intensity for two min every 15 min over a time period of ca. 28 h at 25 °C. We consider the change in the SLS intensity to be negligible during the two-minute period. The measurements started after mixing the two solutions and gently turning the cuvette upside down twice. For comparison, binary aqueous solutions of γ-CD and of the polymers were analyzed by using the same protocol. No time effect was observed for these solutions.

The scattering intensity of the γ-CD–PNIPAAM$_{47}$ mixture increases with time as shown in Fig. 9a. However, during the first 20 min after mixing, the increase is fairly slow (see the inset of

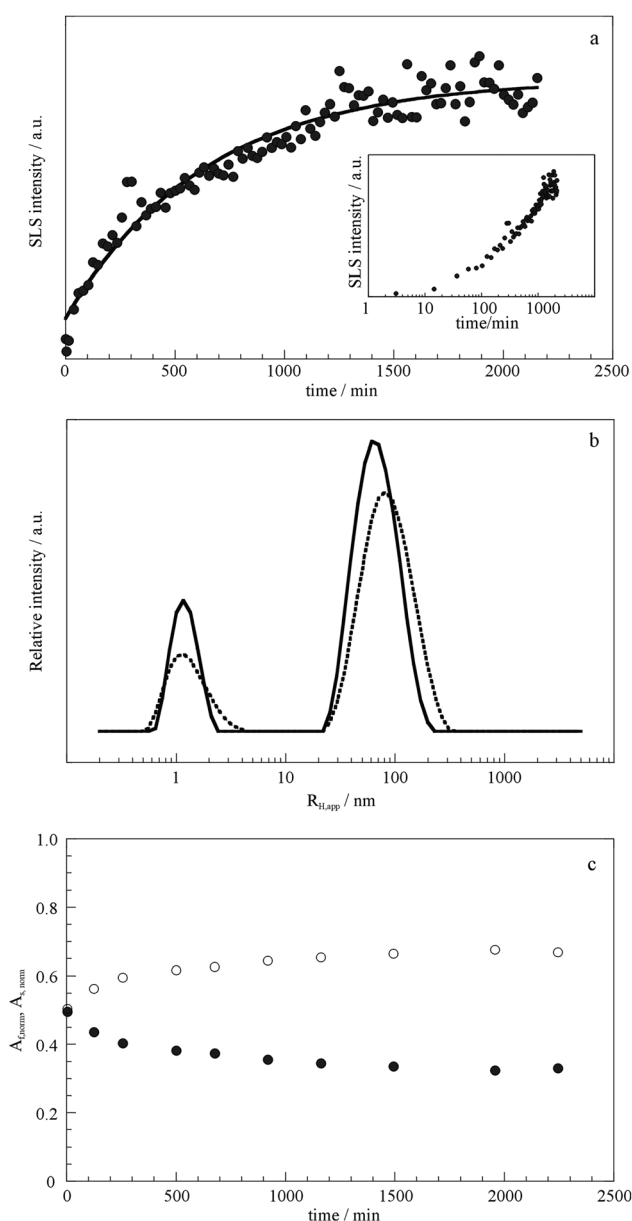**Fig. 9** (a) The total static light scattering intensity as a function of time for an aqueous mixture of 10 wt% γ-CD and 1 wt% PNIPAAM$_{47}$ at 25 °C. The inset shows the intensity against the logarithm of time. (b) Distributions of the apparent hydrodynamic radii after 100 min (dotted line) and 2000 min (solid line) after preparation of the mixed solution. (c) Normalized scattering amplitude of the fast (●) and the slow (○) diffusion mode as a function of time for the same mixture.

Fig. 9a). A slow start has also been observed for a mixture of α-CD and linear PEG using turbidity measurements.[2] This initial region is denoted the threading region, which in turn is a multi-step process.[2]

The molar mass of PNIPAAM plays a key role in the formation of inclusion complexes with γ-CD. The mixture containing the longer PNIPAAM chain (PNIPAAM$_{72}$) did not show any change in the SLS intensity with time (data are reported in the ESI†). The loss of conformational entropy of a long polymer chain upon confinement into a γ-CD tubular structure could be prohibitive.

The data analysis of the DLS correlation functions measured on the γ-CD–PNIPAAM$_{47}$ solution, either by inverse Laplace transformation or by exponential fits, provided new insights. The correlation functions contained two relaxation decays (one fast and one slow). Two intensity-weighted size distributions for the mixed solution at 100 min and at 2000 min after preparation are shown in Fig. 9b. The fast diffusive mode showed a nearly constant $R_{H,app}$ ranging between 1.2 and 1.5 nm (from the bi-exponential fit). For the mixed system, this fast mode can be attributed to translational diffusion of single particles (cyclo-dextrin molecules or homopolymer chains) since the values are comparable to those obtained from the fast mode observed for the γ-CD/water and PNIPAAM$_{47}$/water binary mixtures (1.6 nm and 1.2 nm, respectively). However, it may also be related to the diffusion of inclusion complexes, which are expected to have about the same size as a single homopolymer. $R_{H,app}$ corresponding to the slow mode that is comparable to that of the γ-CD aggregates in water stayed almost constant (between 40 and 50 nm) during the whole experiment. This mode, thus, corresponds to the diffusion of aggregates composed of CD and maybe several γ-CD–PNIPAAM$_{47}$ inclusion complexes.

The normalized relative scattering amplitudes (obtained from the pre-exponential scattering amplitudes in the bi-exponential fit) of the fast and slow modes, $A_{f,norm} = A_f/(A_f + A_s)$ and $A_{s,norm} = A_s/(A_f + A_s)$, respectively, are presented as functions of time in Fig. 9c. We notice that the change with time of the amplitude of the slow mode amplitude is small and that it is always larger than the amplitude of the fast mode. This shows that the scattering originating from the aggregates dominates the total scattering intensity during the whole time of the experiment. Furthermore, the minor increase in $A_{s,norm}$ may reflect an increase in the number of aggregates since the hydrodynamic size of these stays almost constant with time. This conclusion is confirmed by the fact that at a higher concentration (18 wt% of γ-CD), precipitation occurs in a similar way to what has been found for other pseudopolyrotaxane-forming systems.[2]

A completely different time dependence of the SLS intensity was observed for the γ-CD–PNIPAAM$_{24}$-b-PAMPTAM(+)$_9$ copolymer mixture compared to that containing PNIPAAM$_{47}$. In the presence of the copolymer, the SLS intensity was nearly constant for 300 min, thereafter it decreased to reach a plateau after 1600 min (Fig. 10a). This may be compared to the scattering intensity of the γ-CD–PNIPAAM$_{47}$ mixture that changed in the opposite direction with time as shown in Fig. 9a.

The size distributions obtained from ILT of the DLS data for the γ-CD–PNIPAAM$_{24}$-b-PAMPTAM(+)$_9$ mixed solution at 100 min and at 1600 min after preparation are presented in Fig. 10b. The hydrodynamic radii corresponding to the fast diffusive mode are within the range 1.7 ± 0.2 nm to 0.99 ± 0.02 nm, showing a slight decrease with time. $R_{H,app}$ corresponding to the slow mode is larger, 720 ± 20 nm, than those obtained for the aqueous solutions of γ-CD and PNIPAAM$_{24}$-b-PAMPTAM(+)$_9$ 59.4 ± 0.6 nm and 119 ± 1 nm, respectively. All radii values are from bi-exponential fits of the intensity correlation functions. This suggests that large non-equilibrium structures have formed probably due to locally higher concentrations during mixing and their appearance is an artefact from the mixing procedure. The reason for this interpretation is that they disintegrate with time since the SLS intensity decreases as
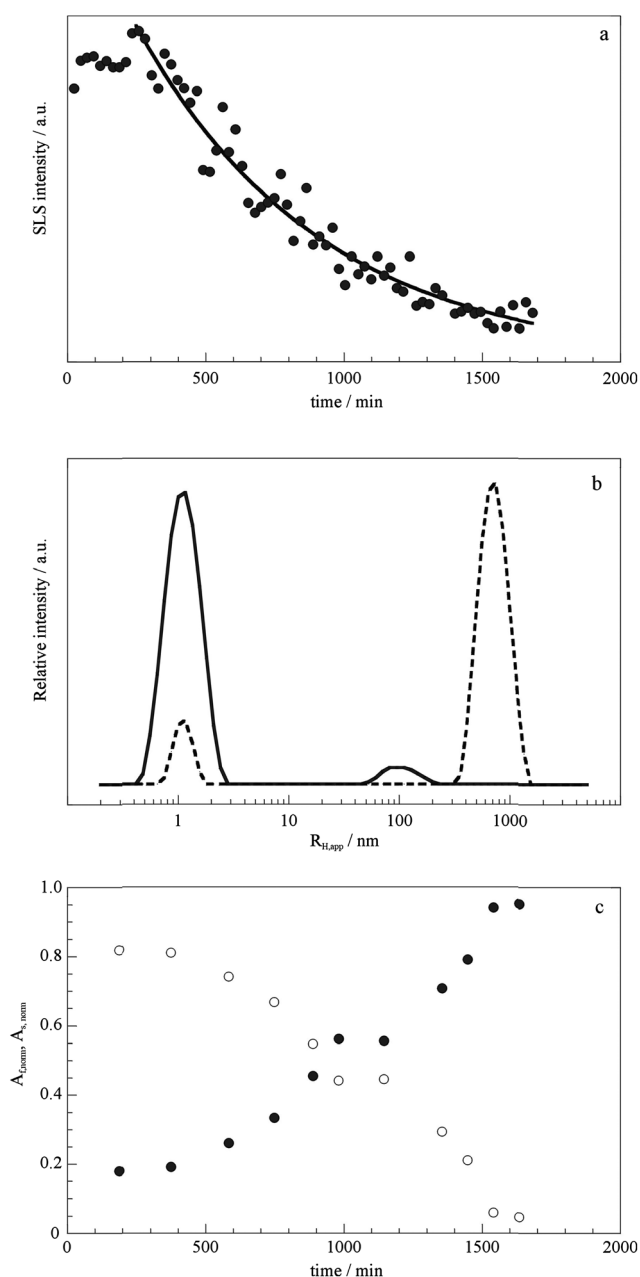
Fig. 10 (a) The total static light scattering intensity as a function of time for an aqueous mixture of 10 wt% γ-CD and 1 wt% copolymer at 25 °C. (b) Distributions of the apparent hydrodynamic radii after 100 min (dotted line) and 1600 min (solid line) after preparation of the mixed solution. (c) Normalized scattering amplitude of the fast (●) and the slow (○) diffusion mode as a function of time for the same mixture.

a function of time (see also discussion of amplitudes below). This means that they are unstable at this total concentration of the solution. It should be stressed that precipitation occurs when the γ-CD concentration exceeds 18 wt%. The non-equilibrium aggregates may be composed of both copolymers and CD aggregates. However they are not ordered in a crystalline structure similar to that of the solid precipitate formed when phase separation occurs at higher CD concentration. The precipitate has a very low solubility at room temperature (see the fluorescence experiments above), whereas these large aggregates

disintegrate. After 1600 min, only objects of the size of CD aggregates, $R_{H,app} = 59 \pm 9$ nm from the bi-exponential fit, are left in equilibrium with small objects. Visual inspection of a solution prepared in a similar manner showed that in the beginning the solution was turbid but it became clear after 12 h. The peculiar time dependence of the γ-CD–PNIPAAM$_{24}$-b-PAMPTAM(+)$_9$ system is also reflected in the normalized relative scattering amplitudes of the fast and slow modes as functions of time (Fig. 10c). $A_{s,norm}$, which is associated with large aggregates, decreases to a very low value with time and the fast diffusive mode dominates almost completely after equilibration at 1600 min, *i.e.* small objects are the main scattering species in the solution. This means as already concluded above that the large non-equilibrium structures have disintegrated. It should be stressed that from the fast mode in the DLS measurements it is not possible to discriminate between the diffusion of free copolymer unimers, free CD molecules and possible inclusion complexes.

The most interesting observation is that the fast amplitude dominates at equilibrium for the γ-CD–copolymer mixture (Fig. 10b), whereas the slow mode dominates in the binary solutions of γ-CD or PNIPAAM$_{24}$-b-PAMPTAM(+)$_9$, see

Fig. 8. This shows that the equilibrium mixture contains fewer CD aggregates due to interactions with the copolymer. The complex aggregates formed by interaction with the block copolymer will break-up due to electrostatic repulsion between the cationic blocks of the copolymer, which are not enclosed in the CD cavities. The effect on the CD self-assembled structures on addition of copolymer is confirmed by cryo-TEM imaging of the mixture at different times, see below.

The crucial role of the proposed electrostatic repulsion between the cationic blocks is confirmed by the time-resolved DLS investigation of the γ-CD–PNIPAAM$_{47}$ mixed solution, where the aggregates observed are constant in size and do not break-up during the time of the experiment (compare Fig. 9 and 10). The repulsive electrostatic effect, which leads to the break-up of the aggregates, is not present in the γ-CD–PNIPAAM$_{47}$ system.

An experiment with a lower copolymer concentration (0.5 wt%) showed an almost negligible change of the scattered intensity with time as well as time-independent amplitudes (data are reported in the ESI†). The copolymer concentration is apparently too low in this mixture to induce formation of the large structures observed at 1 wt% of PNIPAAM$_{24}$-b-PAMPTAM(+)$_9$.
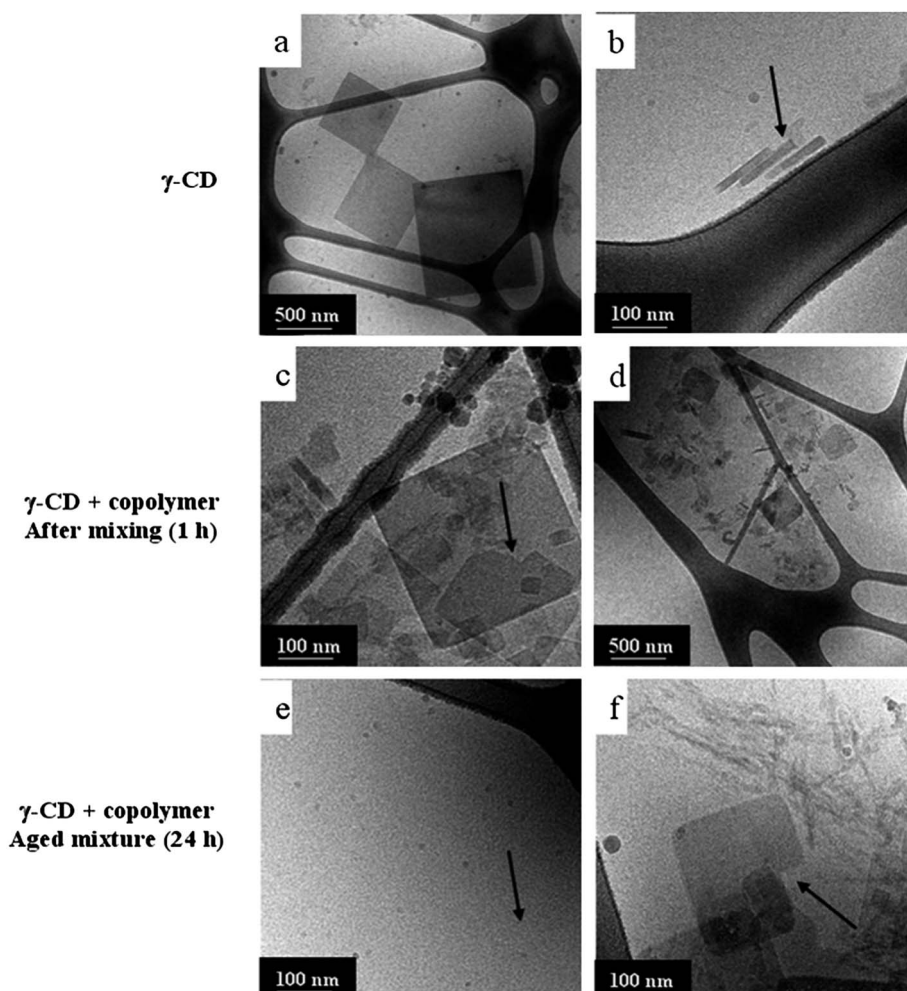

Fig. 11 Cryo-TEM micrographs of the neat γ-CD 10 wt% aqueous solution and of the γ-CD 10 wt% + copolymer 1 wt% mixture in water at different times after mixing. Left- and right-hand columns refer to micrographs from the same sample.

Cryo-TEM

We have performed cryo-TEM experiments on a pure γ-CD solution and a mixed γ-CD–copolymer solution at 1 h and 24 h after preparation. Fig. 11 shows electron micrographs obtained for the samples. Square aggregates were imaged for the 10 wt% γ-CD solution. From a statistical treatment of the images, the ratio between the lengths of two consecutive sides of the aggregates and the angle which they form were found to be 1.03 ± 0.07 and $89 \pm 2°$, respectively. These values indicate a perfect square. However, the size appears rather polydisperse ranging between 1000 and 100 nm. Moreover, rectangular structures were also identified and they possessed a contrast higher than the square structures. It can be concluded that parallelogram structures with a square base are present. It is interesting to note that the height of the parallelogram appears nearly constant, being 20 ± 2 nm.

The addition of 1 wt% of copolymer did not affect the general features exhibited by the neat γ-CD solution if the mixed solution is imaged 1 h after preparation, compare Fig. 11a and b with Fig. 11c and d. However, it can be seen that the corners of the aggregates start to disintegrate after 1 h. The aged mixture give, in addition to the square aggregates with damaged corners, some small objects shown in the micrographs as dots with higher contrast (Fig. 11e and f). It is likely that these are γ-CD–PNIPAAM$_{24}$-b-PAMPTAM(+)$_9$ inclusion complexes. Long strands that seem to be aggregated are visible in Fig. 11f. These may be clusters of inclusion complexes that still are not disintegrated and that co-exist with CD aggregates. However, these cannot be present in large numbers. That in combination with a diminishing form factor at high scattering angles (here 173°) leads to a small contribution to the total light scattering intensity (note the absence of a relaxation mode at long times in the relaxation time distribution at 1600 min in Fig. 10b).

Both cryo-TEM and DLS data show that in 10 wt% γ-CD solution CD aggregates exist with a broad size distribution. These aggregates may have a crucial role in the formation of inclusion complexes as discussed above. However, we have no information from our experimental results on the actual mechanism.

We may conclude that: (1) the γ-CD molecules form self-assembled structures with sizes in the hundred nanometres range; (2) the addition of the copolymer generates smaller objects after several hours; and (3) the rupture of the γ-CD aggregates starts in the corners where the stability is least.

Experimental

Materials

γ-Cyclodextrin (molar mass: 1296 g mol^{-1}), α-cyclodextrin (molar mass: 972 g mol^{-1}), pyrene (99%) and acetone (99.8%) were Aldrich products. D$_2$O (99.8% isotopic purity) was from Armar Chemicals, Döttingen, Switzerland. The cyclodextrins were used as received and their water content was determined by means of thermo-gravimetric analysis (15.3 and 5.2 wt% for γ-cyclodextrin and α-cyclodextrin, respectively). The solutions were prepared by weight using water purified with a Milli-Q system (Millipore Corporation, Bedford, MA). The relative accuracy of the concentrations is 0.01 but the concentrations are referred to as *e.g.* 1 wt% in the text.

Synthesis of poly(*N*-isopropylacrylamide)$_m$

The homopolymers of poly(*N*-isopropylacrylamide) (PNI-PAAM$_m$, where m is the number of monomer repeat units) used in this study were synthesized *via* an ATRP procedure which was described previously.[51] The weight-average molar mass (M_w = 5350 and 9010 g mol^{-1}) and the polydispersity index (M_w/M_n = 1.13 and 1.12) of the two polymer samples were determined by means of asymmetric flow field-flow fractionation (AFFFF) methods. They are denoted PNIPAAM$_{47}$ and PNIPAAM$_{72}$, respectively.[51]

Synthesis of poly(*N*-isopropylacrylamide)$_m$-b-poly((3-acrylamidopropyl)trimethylammonium chloride)$_n$

The copolymer was prepared *via* a simple 'one-pot' two-step ATRP procedure according to our previous report.[53] The preparation and purification of the polymer sample were carried out as described in detail previously.[53,54] The chemical structure and composition of the charged diblock copolymer was ascertained by its ^{1}H-NMR spectrum and the obtained structure is denoted as PNIPAAM$_{24}$-b-PAMPTMA(+)$_9$. A weight-average molar mass of 6080 g mol^{-1} and a fairly narrow molar mass distribution with a polydispersity index M_w/M_n = 1.11 were determined by means of AFFFF methods.[54,55] A copolymer with the composition PNIPAAM$_{26}$-b-PAMPTAM(+)$_{15}$ and with M_n = 6880 g mol^{-1} from ^{1}H-NMR was used in the DSC experiments. Using a polydispersity index of 1.1, we estimate M_w of this polymer to be 7560 g mol^{-1}.

Fourier transform infrared spectroscopy

The FTIR spectra of solid samples dispersed in KBr pellets were measured with a Bruker IFS 66 spectrometer. The explored range was from 4000 cm^{-1} to 400 cm^{-1} and the spectral resolution was 2 cm^{-1}. The average values of 128 repeated scans are reported.

^{1}H-NMR

The NMR measurements were carried out by using a Bruker DRX 400 MHz spectrometer operating at 25.0 ± 0.1 °C. Proton chemical shifts (δ) of the homo- and copolymer and cyclodextrin were referenced to the proton of the HDO (δ = 4.7 ppm) peak. The solutions for NMR measurements were prepared in D$_2$O by weight one day prior to the measurements. The precision in the chemical shift measurements is estimated to be at least ± 0.001 ppm. Chart 1 illustrates the molecular structure of the polymers investigated in this study and γ-CD as well as the numbering of the different ^{1}H nuclei that were selected for the data analysis.

Synchrotron radiation powder X-ray diffraction

The SR-PXD data were collected at beamline I911-5 of the synchrotron MAX II, Lund, Sweden.[56] The X-ray exposure time was 10 s and the wavelength was 0.9077 Å. All raw images were analyzed using the FIT2D program.[57] Calibration measurements were carried out using a LaB$_6$ sample. Sample-to-detector distances of 50, 100, 200, 300, and 380 mm were used to cover a wide range of the scattering vector $q = 4\pi\lambda^{-1}\sin(\theta/2)$, where λ denotes the wavelength and θ the scattering angle.

Steady-state fluorescence spectroscopy

Steady-state pyrene fluorescence emission spectra of air-equilibrated solutions were recorded in steps of 1 nm with an integration time of 1 s with a Varian, Cary Eclipse spectrofluorometer (right angle geometry, 1 cm × 1 cm quartz cell) at 20 °C and 40 °C. The temperature was controlled to within ± 0.1 °C. The intensity was measured against the reference signal of the lamp and the baseline was subtracted. The excitation wavelength was set at 333 nm and the emission spectra from 350 nm to 500 nm were recorded. The slit width was 2.5 nm for both excitation and emission. The pyrene solution was prepared as described previously.[58] The final pyrene concentration was 5×10^{-7} mol dm^{-3}, which is close to its solubility in water. Excimer emission (at longer wavelength) was not observed due to the low pyrene concentration.

Differential scanning calorimetry

The temperature-induced self-assembly of the polymers in water and in water in the presence of γ-CD was monitored by means of a VP-DSC (Microcal) in the 5 °C to 75 °C temperature range at a heating rate of 0.6 °C min^{-1}. The sample cell was filled with 0.507 cm^3 of the aqueous solution while the reference cell was filled with water. The baseline was subtracted as described in the literature.[59]

Dynamic and static light scattering

DLS and SLS measurements were performed using a Zetasizer Nano ZS instrument equipped with the DTS Ver. 5.03 (Malvern Instruments Ltd., Worcestershire, UK) software package, at a fixed scattering angle of 173° by means of the non-invasive backscatter detection technology.[60] A He–Ne laser (4 mW) with a wavelength of 632.8 nm is used as the light source and the detection unit comprises an avalanche photodiode. The solvent used was filtered through 0.22 mm Millipore filters.

The normalized form of the measured intensity autocorrelation function $g^{(2)}(t)$ is related to the normalized autocorrelation function of the electric field $g^{(1)}(t)$ via the Siegert relation, $g^{(2)}(t) - 1 = \beta|g^{(1)}(t)|^2$, where coherence factor β takes into account experimental deviations from ideal correlation. The $g^{(2)}(t) - 1$ functions were analyzed using two procedures. In the first method, the intensity correlation function was fitted by means of two exponential decays in order to determine two characteristic relaxation times (τ) and the corresponding pre-exponential scattering amplitudes (A_f and A_s for the fast and the slow diffusive mode, respectively): $g^{(2)}(t) - 1 = A_f \exp(-2t/\tau_f) + A_s \exp(-2t/\tau_s)$ + baseline. For the translational motion, the mutual (or collective) diffusion coefficient at finite concentrations is given by $D = q^2\tau^{-1}$, where q denotes the magnitude of the scattering vector (here $q = 4\pi n\lambda^{-1}\sin(\theta/2)$ in which n is taken as the refractive index of water). From D, the apparent hydrodynamic radius $R_{H,app}$ may be calculated using the Stokes–Einstein equation and the water viscosity at the corresponding temperature.

In the second method a computer algorithm of the Malvern software, which performs an inverse Laplace transformation (ILT), was employed. This type of analysis may be used for systems containing a range of particle sizes and, thus, the correlation function will exhibit a multiexponential decay. The ILT analysis yields an intensity-weighted relaxation time distribution $A(\tau)$, which easily can be transformed to an intensity-weighted particle size distribution based on the apparent hydrodynamic radii. The two different procedures provided values of the hydrodynamic radii that are in a good agreement. This corroborates the reliability of the obtained results.

Cryo-transmission electron microscopy

The samples were prepared in a controlled environment vitrification system (CEVS), at 20 °C.[61] A 5 µL drop of sample solution was placed on a lacey carbon-coated copper grid made hydrophilic using an Emitech glow discharge unit. The excess fluid was gently blotted away leaving a thin film of aqueous sample covering the grid. Liquid ethane at −180 °C was used to allow rapid vitrification of the specimen (avoiding crystallization of water) and the grids were stored in liquid nitrogen until they were transferred to the electron microscope. Transmission electron micrographs were digitally recorded using a Philips CM120 Bio TWIN electron microscope, operated at 120 kV, equipped with a Gatan MSC791 cooled-CCD camera system. Minimal electron dose conditions were used to minimize beam damage of the samples.

Conclusions and outlook

The temperature-responsive cationic diblock copolymer PNIPAAM$_{24}$-b-PAMPTAM(+)$_9$ and the PNIPAAM homopolymer PNIPAAM$_{47}$ form inclusion complexes with γ-cyclodextrin at 25 °C in aqueous solution. The CD molecules thread the PNIPAAM chain as well as the PNIPAAM block of the copolymer but the bulky cationic block is not incorporated into the CD cavity. The stoichiometry of the γ-CD–polymer inclusion complexes was found to be close to two NIPAAM units per CD molecule, which confirms a close packing of the CDs. The observation of a precipitate in the mixed CD–copolymer solutions at high CD concentrations confirms that inclusion complexes also are formed in the solid state. The proposed structure of the two solid inclusion complexes is columnar with a head-to-head and tail-to-tail arrangement of the CD molecules. Dynamic light scattering and cryo-TEM experiments reveal that square-shaped aggregates of γ-CD co-exist with single CD molecules in water. The time-resolved SLS and DLS measurements demonstrate that in γ-CD–PNIPAAM$_{24}$-b-PAMPTAM(+)$_9$ mixtures the CD aggregates disintegrate with time, which leads to an increased amount of inclusion complexes in the solution.

A change in temperature significantly influences the inclusion-complex system, which suggests the possibility of the design of thermosensitive systems based on PNIPAAM pseudopolyrotaxanes. When the temperature approaches the LCST of PNIPAAM, the CD molecules dethread from the PNIPAAM block of PNIPAAM$_{24}$-b-PAMPTAM(+)$_9$ or from PNIPAAM$_{47}$ as disclosed from steady-state fluorescence measurements. The mechanism behind the threading/dethreading phenomenon will therefore be an interesting issue for future theoretical model calculations of polymer configurations in confined space.

The specific thermoresponsive behavior that we have observed for the CD-inclusion-complex systems investigated in this work can also be observed at solid–liquid interfaces. The adsorption of PNIPAAM$_n$-b-PAMPTMA(+)$_m$ copolymers at the silica–water interface and the effect of the inclusion of the PNIPAAM chains in γ-CD molecules are currently the subject of a detailed investigation using null ellipsometry, quartz crystal microbalance with dissipation monitoring and neutron reflectometry measurements. The adsorbed copolymer layer is characterized in the absence and presence of γ-CD molecules at temperatures below and above the LCST of PNIPAAM.[62]

Acknowledgements

References

1 G. Wenz, B.-H. Han and A. Müller, *Chem. Rev.*, 2006, **106**, 782–817.
2 P. Lo Nostro, L. Giustini, E. Fratini, B. W. Ninham, F. Ridi and P. Baglioni, *J. Phys. Chem. B*, 2008, **112**, 1071–1081.
3 F. Yuen and K. C. Tam, *Soft Matter*, 2010, **6**, 4613–4630.
4 D. F. Evans and H. Wennerström, *The Colloidal Domain: where Physics, Chemistry, Biology and Technology Meet*, John Wiley & Sons, Inc., New York, 1999.
5 J. Araki and K. Ito, *Soft Matter*, 2007, **3**, 1456–1473.
6 G. Lazzara and S. Milioto, *J. Phys. Chem. B*, 2008, **112**, 11887–11895.
7 H. Fujita, T. Ooya and N. Yui, *Macromolecules*, 1999, **32**, 2534–2541.
8 M. Bonini, S. Rossi, G. Karlsson, M. Almgren, P. Lo Nostro and P. Baglioni, *Langmuir*, 2006, **22**, 1478–1484.
9 Y. F. He, P. Fu, X. H. Shen and H. C. Gao, *Micron*, 2008, **39**, 495–516.
10 S. Polarz, B. Smarsly, L. Bronstein and M. Antonietti, *Angew. Chem., Int. Ed.*, 2001, **40**, 4417–4421.
11 M. Wei, W. Davis, B. Urban, Y. Q. Song, F. E. Porbeni, X. W. Wang, J. L. White, C. M. Balik, C. C. Rusa, J. Fox and A. E. Tonelli, *Macromolecules*, 2002, **35**, 8039–8044.
12 H. Goto, Y. Furusho and E. Yashima, *J. Am. Chem. Soc.*, 2007, **129**, 109–112.
13 Y. Xu, S. Bolisetty, M. Ballauff and A. H. E. Müller, *J. Am. Chem. Soc.*, 2009, **131**, 1640–1641.
14 J. X. Zhang, H. L. Sun and P. X. Ma, *ACS Nano*, 2010, **4**, 1049–1059.
15 Y. Liu, L. Yu, Y. Chen, Y. L. Zhao and H. Yang, *J. Am. Chem. Soc.*, 2007, **129**, 10656–10657.
16 F. Cacialli, J. S. Wilson, J. J. Michels, C. Daniel, C. Silva, R. H. Friend, N. Severin, P. Samorì, J. P. Rabe, M. J. O'Connell, P. N. Taylor and H. L. Anderson, *Nat. Mater.*, 2002, **1**, 160–164.
17 G. G. Gaitano, W. Brown and G. Tardajos, *J. Phys. Chem. B*, 1997, **101**, 710–719.
18 S. Schmitz and H. Ritter, *Angew. Chem., Int. Ed.*, 2005, **44**, 5658–5661.
19 J. Joseph, C. A. Dreiss, T. Cosgrove and J. S. Pedersen, *Langmuir*, 2007, **23**, 460–466.
20 R. De Lisi and G. Lazzara, *J. Therm. Anal. Calorim.*, 2009, **97**, 797–803.
21 G. Lazzara, S. Prevost and M. Gradzielski, *Soft Matter*, 2011, **7**, 6082–6091.
22 M. Valero, I. Grillo and C. A. Dreiss, *J. Phys. Chem. B*, 2012, **116**, 1273–1281.
23 H. Ritter, O. Sadowski and E. Tepper, *Angew. Chem., Int. Ed.*, 2003, **42**, 3171–3173.
24 S. J. Han, M. K. Yoo, Y. K. Sung, Y. M. Lee and C. S. Cho, *Macromol. Rapid Commun.*, 1998, **19**, 403–407.
25 M. L. Patrizi, M. Diociaiuti, D. Capitani and G. Masci, *Polymer*, 2009, **50**, 467–474.
26 E. Sabadini, T. Cosgrove and F. d. C. Egídio, *Carbohydr. Res.*, 2006, **341**, 270–274.
27 A. Harada, J. Li and M. Kamachi, *Macromolecules*, 1993, **26**, 5698–5703.
28 A. Harada and M. Kamachi, *Macromolecules*, 1990, **23**, 2821–2823.
29 J. Li, D. Yan, X. Jiang and Q. Chen, *Polymer*, 2002, **43**, 2625–2629.
30 A. Harada, J. Li and M. Kamachi, *Nature*, 1992, **356**, 325–327.
31 J. Y. Li, Y. Y. Mai, D. Y. Yan and Q. Chen, *Colloid Polym. Sci.*, 2003, **281**, 267–274.
32 J. Li, X. P. Ni, Z. H. Zhou and K. W. Leong, *J. Am. Chem. Soc.*, 2003, **125**, 1788–1795.
33 M. V. Rekharsky and Y. Inoue, *Chem. Rev.*, 1998, **98**, 1875–1917.
34 L. Lepori and P. Gianni, *J. Solution Chem.*, 2000, **29**, 405–447.
35 W. K. Zhang, S. Zou, C. Wang and X. Zhang, *J. Phys. Chem. B*, 2000, **104**, 10258–10264.
36 G. Fronza, A. Mele, E. Redenti and P. Ventura, *J. Org. Chem.*, 1996, **61**, 909–914.
37 M. V. Rekharsky, F. P. Schwarz, Y. B. Tewari, R. N. Goldberg, M. Tanaka and Y. Yamashoji, *J. Phys. Chem.*, 1994, **98**, 4098–4103.
38 V. K. Smith, T. T. Ndou and I. M. Warner, *J. Phys. Chem.*, 1994, **98**, 8627–8631.
39 S. Crouzy, F. Fauvelle, J. C. Debouzy, M. Goschl and Y. Chapron, *Carbohydr. Res.*, 1996, **287**, 21–35.
40 J. Zhang and N. A. Peppas, *J. Appl. Polym. Sci.*, 2001, **82**, 1077–1082.
41 C. C. Rusa, T. A. Bullions, J. Fox, F. E. Porbeni, X. W. Wang and A. E. Tonelli, *Langmuir*, 2002, **18**, 10016–10023.
42 M. A. Hunt, C. C. Rusa, A. E. Tonelli and C. M. Balik, *Carbohydr. Res.*, 2005, **340**, 1631–1637.
43 J. Kawasaki, D. Satou, T. Takagaki, T. Nemoto and A. Kawaguchi, *Polymer*, 2007, **48**, 1127–1138.
44 A. Altomare, R. Caliandro, M. Camalli, C. Cuocci, C. Giacovazzo, A. G. G. Moliterni and R. Rizzi, *J. Appl. Crystallogr.*, 2004, **37**, 1025–1028.
45 D. C. Dong and M. A. Winnik, *Rev. Can. Chim.*, 1984, **62**, 2560–2565.
46 H. G. Schild, *Prog. Polym. Sci.*, 1992, **17**, 163–249.
47 F. Eeckman, K. Amighi and A. J. Moes, *Int. J. Pharm.*, 2001, **222**, 259–270.
48 H. G. Schild and D. A. Tirrell, *Langmuir*, 1991, **7**, 665–671.
49 R. De Lisi, G. Lazzara, S. Milioto and N. Muratore, *Phys. Chem. Chem. Phys.*, 2003, **5**, 5084–5090.
50 R. De Lisi, S. Milioto, A. De Giacomo and A. Inglese, *Langmuir*, 1999, **15**, 5014–5022.
51 R. Pamies, K. Z. Zhu, A. L. Kjøniksen and B. Nyström, *Polym. Bull.*, 2009, **62**, 487–502.
52 T. Costa, J. S. de Melo, M. d. G. Miguel, B. Lindman and K. Schillén, *J. Phys. Chem. B*, 2009, **113**, 6205–6214.
53 A.-L. Kjøniksen, K. Zhu, R. Pamies and B. Nyström, *J. Phys. Chem. B*, 2008, **112**, 3294–3299.
54 R. Pamies, K. Zhu, S. Volden, A.-L. Kjøniksen, G. Karlsson, W. R. Glomm and B. Nyström, *J. Phys. Chem. C*, 2010, **114**, 21960–21968.
55 K. Zhu, H. Jin, A.-L. Kjøniksen and B. Nyström, *J. Phys. Chem. B*, 2007, **111**, 10862–10870.
56 C. B. Mammen, T. Ursby, Y. Cerenius, M. Thunnissen, J. Als-Nielsen, S. Larsen and A. Liljas, *Acta Phys. Pol., A*, 2002, **101**, 595–602.
57 A. P. Hammersley, S. O. Svensson, M. Hanfland, A. N. Fitch and D. Hausermann, *High Pressure Res.*, 1996, **14**, 235–248.
58 G. Lazzara, S. Milioto and M. Gradzielski, *Phys. Chem. Chem. Phys.*, 2006, **8**, 2299–2312.
59 D. V. Malakhov and M. K. A. Khatwa, *J. Therm. Anal. Calorim.*, 2007, **87**, 595–599.
60 D. Lundberg, A. M. Carnerup, K. Schillén, M. d. G. Miguel and B. Lindman, *Langmuir*, 2010, **26**, 2986–2988.
61 J. R. Bellare, H. T. Davis, L. E. Scriven and Y. Talmon, *J. Electron Microsc. Tech.*, 1988, **10**, 87–111.
62 G. Lazzara, N. Reichhardt, R. A. Campbell, S. Bayati, K. Zhu, B. Nyström, T. Nylander and K. Schillén, manuscript in preparation.